



Title	Thermodynamic stability boundaries and structures of methane + monohalogenated cyclopentane mixed hydrates
Author(s)	Matsumoto, Yuuki; Matsukawa, Hiroaki; Kamo, Fumitaka et al.
Citation	Journal of Chemical and Engineering Data. 2014, 59(7), p. 2294-2297
Version Type	AM
URL	https://hdl.handle.net/11094/100986
rights	© 2014 American Chemical Society.
Note	

The University of Osaka Institutional Knowledge Archive : OUKA

<https://ir.library.osaka-u.ac.jp/>

The University of Osaka

Thermodynamic Stability Boundaries and Structures of Methane+Monohalogenated Cyclopentane Mixed Hydrates

*Yuuki Matsumoto¹, Hiroaki Matsukawa¹, Fumitaka Kamo¹, Young Bae Jeon¹, Yoshito Katsuta¹,
Tatsuya Bando¹, Takashi Makino², Takeshi Sugahara^{1,*} and Kazunari Ohgaki¹.*

¹ Division of Chemical Engineering, Department of Materials Engineering Science, Graduate School of Engineering Science, Osaka University, 1-3 Machikaneyama, Toyonaka, Osaka 560-8531, Japan

² National Institute of Advanced Industrial Science and Technology, 4-2-1 Nigatake, Miyagino, Sendai, Miyagi 983-8551, Japan

ABSTRACT

Thermodynamic stability boundaries of the mixed hydrate composed of methane and fluorocyclopentane, chlorocyclopentane, or bromocyclopentane were investigated in a temperature range of (274.17 to 306.19) K and pressures up to 9.93 MPa under the four-phase (hydrate, aqueous, monohalogenated cyclopentane-rich liquid, and gas phases) equilibrium

conditions. Also, the crystal structure of the methane+chlorocyclopentane hydrate was determined by means of powder X-ray diffractometry. The each boundary is laid at a pressure lower and a temperature higher than that of the simple methane hydrate. Especially, the methane+fluorocyclopentane hydrate system has the lowest equilibrium pressure among three mixed hydrate systems investigated in the present study. The powder X-ray diffraction patterns reveal that a guest species larger than chrolocyclopentane and smaller than bromocyclopentane is border between structure-II and structure-H hydrate formers.

Keywords: Clathrate hydrate, Phase equilibria, Powder X-ray diffractometry, Cage occupancy

INTRODUCTION

Clathrate hydrate is a solid crystalline, which has an ice-like appearance. Hydrate is necessarily composed of water (host) and guest species such as light hydrocarbons and noble gases. The water molecules construct cage structure and one cage normally enclathrates one guest molecule. The existence of several kinds of hydrate cages has been reported. For instance, 5^{12} -cage (S-cage) is a dodecahedron, which is constructed from twelve (12) pentagons (5). $4^35^66^3$ -cage (S'-cage), $5^{12}6^2$ -cage (M-cage), $5^{12}6^4$ -cage (L-cage), and $5^{12}6^8$ -cage (U-cage) follow the same rule. Some of them are combined to form specific hydrate structures. The unit cell of the structure-I (s-I) hydrate consists of two S-cages and six M-cages. In the same manner, that of the structure-II (s-II) hydrate is formed with 16 S-cages and eight L-cages. The unit cell of the structure-H (s-H) hydrate is composed of three S-cages, two S'-cages, and one U-cage. Simple

hydrate is formed with a binary mixture that is water and single guest species. On the other hand, mixed hydrate is formed with more than ternary mixture that is water and more than two kinds of guest species. Crystal structures and thermodynamic stabilities of hydrates depend on the thermodynamic condition (pressure, temperature, composition, etc.) and the properties of guest species (size, shape, molar volume, molar weight, solubility, polarity, etc.).^{1,2} Some of large guest species (LGS) cannot form hydrates solely. When a small guest species such as methane (CH₄) is added, such LGSs occupy the L-cage of s-II hydrate or the U-cage of s-H hydrate with support of the S-cage (and S'-cage) occupancy of a small guest species. In this case, the small guest species is called “help gas”. In the case of s-H hydrate, the combination ratio of small cages to large cages in the unit lattice is larger than those of s-I and s-II hydrates, and the S'-cage and the U-cage have geometrically unstable faces (squares and hexagons). Therefore, the contribution of help gases occupying the S- and S'-cages is necessary to form s-H hydrates.³

Hydrate enclathrates a large amount of gases such as CH₄ and carbon dioxide (CO₂). Therefore, hydrate is suggested to be utilized for gas storage, transportation, and separation. However, high pressure and/or low temperature are required for the formation and stabilization of hydrates, which is one of the most serious problems to be solved. Adding an LGS as a thermodynamic promoter to a simple gas hydrate system, gas and LGS occupy small and large cages respectively, resulting that s-II or s-H mixed hydrate can form at thermodynamic conditions milder than simple gas hydrate (i.e. lower pressure and higher temperature). In addition, the ratios of small to large cages in the s-II (the ratio is 2.0) and s-H (5.0) unit lattices are much larger than that in the s-I unit lattice (1/3). That is why s-II and s-H hydrates have attracted attention in the field of natural gas storage and transport. So far, many LGSs forming s-II and s-H mixed hydrates with a help gas have been reported.¹ We reported that cyclopentane (*c*-

C_5H_{10}) and fluorocyclopentane (*c*- C_5H_9F) form the s-II mixed hydrates with CO_2 .⁴ However, the occupancy limit for the L-cage of s-II hydrate has not been clarified yet. Which cage LGSs occupy is fundamentally significant in revealing the occupancy limits of LGSs for the L-cage of s-II hydrate.

In the present study, three kinds of monohalogenated cyclopentanes (*c*- C_5H_9X , X = F, Cl, and Br) are adopted as LGSs. The four-phase (hydrate, aqueous, *c*- C_5H_9X -rich liquid, and gas phases) equilibrium curves of the CH_4+c - C_5H_9F , CH_4+c - C_5H_9Cl , and CH_4+c - C_5H_9Br mixed hydrate systems were measured. The structures of the CH_4+c - C_5H_9Cl and CH_4+c - C_5H_9Br mixed hydrates, in addition, were clarified based on powder X-ray diffraction (PXRD) pattern.

EXPERIMENTAL

Materials. Materials used in the present study are summarized in Table 1. All of them were used without further purification.

Apparatus. The high-pressure cell (inner volume: 150 cm³, maximum working pressure: 10 MPa) used in the present study is the same as the one used previously.⁵ The system temperature was controlled with the thermocontroller (Taitec, CL-80R). The equilibrium temperature was measured with the thermistor thermometer (Takara, D632, reproducibility: 0.02 K). The equilibrium pressure was measured with the pressure gauges (Valcom, VPRT, maximum uncertainties: 0.04 MPa). PXRD patterns were obtained with a diffractometer (Rigaku, Ultima IV) with a Rigaku D/teX ultra high-speed position sensitive detector and $CuK\alpha$ X-ray (generation power: 40 kV, 50 mA).

Procedure. Sufficient amount of distilled water and *c*-C₅H₉X (X = F, Cl, and Br) was introduced into the high-pressure cell. These two liquids of water and *c*-C₅H₉X are not completely miscible at pressures, temperatures, and compositions in the present study, that is, aqueous and *c*-C₅H₉X-rich liquid phases coexist. The cell was immersed in the thermostatic bath. After the air dissolved in water and *c*-C₅H₉X was deaerated, the contents were pressurized with CH₄ up to the desired pressure. The contents were cooled with the thermocontroller and agitated with continuously-moving magnetic stirrer to generate hydrates effectively. After the formation of hydrates, temperature was increased up to a desired temperature and kept constant to establish the four-phase (hydrate, aqueous, *c*-C₅H₉X-rich liquid, and gas phases) equilibrium condition. When a four-phase equilibrium condition was established, pressure and temperature were recorded as an equilibrium datum set. Please note that the system pressure was controlled not to exceed the equilibrium pressure of the simple CH₄ hydrate at given temperature during all of the process mentioned above.

For the PXRD analysis, after the four-phase equilibrium condition was established in the CH₄+*c*-C₅H₉Cl and CH₄+*c*-C₅H₉Br mixed hydrate systems, the contents were pressurized with additional CH₄ so that almost all of free water was converted to mixed hydrate. The hydrate samples were taken from the cell at 263 K and kept at 77 K. Samples were ground and set flatly on the sample stage of the diffractometer. PXRD patterns were measured at 143 K. The measurements were performed in the stepscan mode with step size of 0.02°. The PXRD pattern indexing and cell refinement were obtained with the Chekcell⁶ and PowderX⁷ programs and the initial lattice parameters for the refinement.

RESULTS AND DISCUSSION

The PXRD patterns of the $\text{CH}_4+c\text{-C}_5\text{H}_9\text{Cl}$ and $\text{CH}_4+c\text{-C}_5\text{H}_9\text{Br}$ mixed hydrates obtained in the present study are shown in Figure 1. The typical pattern of s-II hydrate was observed in the $\text{CH}_4+c\text{-C}_5\text{H}_9\text{Cl}$ mixed hydrate. The space group and the lattice constant (a) of the $\text{CH}_4+c\text{-C}_5\text{H}_9\text{Cl}$ mixed hydrate are $Fd3m$ and $a = (1.734 \pm 0.003)$ nm (prepared at 1.93 MPa and 277.89 K, measured at 143 K), respectively, which elucidate that $c\text{-C}_5\text{H}_9\text{Cl}$ was enclathrated into the L-cage of s-II hydrate in the presence of CH_4 . On the other hand, the typical pattern of s-H hydrate was detected in the $\text{CH}_4+c\text{-C}_5\text{H}_9\text{Br}$ mixed hydrate as reported previously¹⁰. The space group and the lattice constants (a and c) of the $\text{CH}_4+c\text{-C}_5\text{H}_9\text{Br}$ mixed hydrate are $P6/mmm$ and $a = (1.232 \pm 0.001)$ nm, $c = (1.019 \pm 0.001)$ nm (prepared at 1.82 MPa and 274.17 K, measured at 143 K), respectively. The PXRD patterns also reveal that there is the limit of L-cage occupancy between $c\text{-C}_5\text{H}_9\text{Cl}$ and $c\text{-C}_5\text{H}_9\text{Br}$, the former is one of the largest LGSs that occupy the L-cage of s-II hydrate and the latter is one of the smallest LGSs that occupy the U-cage of s-H hydrate.

Thermodynamic stability boundaries of $\text{CH}_4+c\text{-C}_5\text{H}_9\text{X}$ ($\text{X} = \text{F}$, Cl , and Br) mixed hydrates measured in the present study under the four-phase (hydrate, aqueous, $c\text{-C}_5\text{H}_9\text{X}$ -rich liquid, and gas phases) equilibrium conditions are shown in Figure 2 accompanied with those of the s-II $\text{CH}_4+c\text{-C}_5\text{H}_{10}$ mixed hydrate^{8,9} and the s-I simple CH_4 hydrate.⁵ The obtained four-phase equilibrium data are also listed in Table 2. The data in the $\text{CH}_4+c\text{-C}_5\text{H}_9\text{Br}$ mixed hydrate agree well with the data recently reported.¹⁰ The four-phase equilibrium curves are located at a lower pressure and higher temperature side than the three-phase (hydrate, aqueous, and gas phases) equilibrium curve of the s-I simple CH_4 hydrate system. All of the $c\text{-C}_5\text{H}_9\text{X}$ adopted in the present study work as thermodynamic promoters. The s-II $\text{CH}_4+c\text{-C}_5\text{H}_9\text{F}$ mixed hydrate is the most thermodynamically stable in the present study, followed by the s-II $\text{CH}_4+c\text{-C}_5\text{H}_9\text{Cl}$ and the

s-H $\text{CH}_4+c\text{-C}_5\text{H}_9\text{Br}$ mixed hydrates. Thermodynamic stability region of the s-II $\text{CH}_4+c\text{-C}_5\text{H}_9\text{F}$ mixed hydrate is quite different from that of the s-II $\text{CH}_4+c\text{-C}_5\text{H}_9\text{Cl}$ mixed hydrate. It implies that $c\text{-C}_5\text{H}_9\text{F}$ has a quite suitable molecular size and shape for the L-cage occupancy, whereas $c\text{-C}_5\text{H}_9\text{Cl}$ may be a little bit too large for the L-cage occupancy. Especially, the $\text{CH}_4+c\text{-C}_5\text{H}_9\text{F}$ hydrate is formed at thermodynamic conditions milder than $\text{CH}_4+c\text{-C}_5\text{H}_{10}$ hydrate,^{8,9} although it has been considered that $c\text{-C}_5\text{H}_{10}$ is one of the best thermodynamic promoters for the CH_4 enclathration. The same tendency is observed in the $\text{Kr}+c\text{-C}_5\text{H}_{10}$ and $\text{Kr}+c\text{-C}_5\text{H}_9\text{F}$ mixed hydrates,^{11,12} $\text{CH}_3\text{F}+c\text{-C}_5\text{H}_{10}$ and $\text{CH}_3\text{F}+c\text{-C}_5\text{H}_9\text{F}$ mixed hydrates,¹³ $\text{CH}_2\text{F}_2+c\text{-C}_5\text{H}_{10}$ and $\text{CH}_2\text{F}_2+c\text{-C}_5\text{H}_9\text{F}$ mixed hydrates,^{12,14} and $\text{CO}_2+c\text{-C}_5\text{H}_{10}$ and $\text{CO}_2+c\text{-C}_5\text{H}_9\text{F}$ mixed hydrates.⁴

CONCLUSIONS

Thermodynamic stabilities of $\text{CH}_4+c\text{-C}_5\text{H}_9\text{F}$, $\text{CH}_4+c\text{-C}_5\text{H}_9\text{Cl}$, and $\text{CH}_4+c\text{-C}_5\text{H}_9\text{Br}$ mixed hydrate systems were investigated. In addition, the structure of these mixed hydrates was clarified. Compared to the s-I simple CH_4 hydrate, the s-II $\text{CH}_4+c\text{-C}_5\text{H}_9\text{F}$ mixed hydrate is much more thermodynamically stable, followed by the s-II $\text{CH}_4+c\text{-C}_5\text{H}_9\text{Cl}$, and the s-H $\text{CH}_4+c\text{-C}_5\text{H}_9\text{Br}$ mixed hydrates. $c\text{-C}_5\text{H}_9\text{F}$ works as a thermodynamic promoter much greater than $c\text{-C}_5\text{H}_{10}$, $c\text{-C}_5\text{H}_9\text{Cl}$, and $c\text{-C}_5\text{H}_9\text{Br}$. The limit of L-cage occupancy is located between $c\text{-C}_5\text{H}_9\text{Cl}$ and $c\text{-C}_5\text{H}_9\text{Br}$.

AUTHOR INFORMATION

Corresponding Author

* Tel.&Fax.: +81-6-6850-6293. E-mail: sugahara@cheng.es.osaka-u.ac.jp.

Notes

The authors declare no competing financial interest.

ACKNOWLEDGEMENTS

This work was partially supported by KAKENHI, Grant-in-Aid for JSPS Fellows (25·1430) (YM), Grant-in-Aid for Young Research (B) (22710081) (TM) and the Kansai Research Foundation for technology promotion (TM). We acknowledge the scientific support from the “Gas-Hydrate Analyzing System (GHAS)” of Division of Chemical Engineering, Department of Materials Engineering Science, Graduate School of Engineering Science, Osaka University.

REFERENCES

- (1) Sloan, E.D.; Koh, C.A. *Clathrate Hydrates of Natural Gases*, 3rd ed.; Taylor & Francis-CRC Press: Boca Raton, FL, 2008.
- (2) Tezuka, K.; Taguchi, T.; Alavi, S.; Sum, A.K.; Ohmura, R. Thermodynamic Stability of Structure H Hydrates Based on the Molecular Properties of Large Guest Molecules. *Energies* **2012**, *5*, 459–465.
- (3) Ripmeester, J.A.; Tse, J.S.; Ratcliffe, C.I.; Powell, B.M. A New Clathrate Hydrate Structure. *Nature* **1987**, *325*, 135–136.

(4) Matsumoto, Y.; Makino, T.; Sugahara, T.; Ohgaki, K. Phase Equilibrium Relations for Binary Mixed Hydrate Systems Composed of Carbon Dioxide and Cyclopentane Derivatives. *Fluid Phase Equilib.* **2014**, *362*, 379–382.

(5) Nakamura, T.; Makino, T.; Sugahara, T.; Ohgaki, K. Stability Boundaries of Gas Hydrates Helped by Methane – Structure-H Hydrates of Methylcyclohexane and *cis*-1,2-Dimethylcyclohexane. *Chem. Eng. Sci.* **2003**, *58*, 269–273.

(6) Chekcell; <http://www ccp14.ac.uk>. Chekcell developed by Laugier, L.; Bochu, B. Laboratoire des Materiaux et du Genie Physique, Ecole Supérieure de Physique de Grenoble: Grenoble, France (accessed April 28, 2011).

(7) Dong, C. PowderX: Windows-95-based Program for Powder X-ray Diffraction Data Processing. *J. Appl. Crystallogr.* **1999**, *32*, 838.

(8) Tohidi, B.; Danesh, A.; Todd, A.C.; Burgass, R.W.; Østergaard, K.K. Equilibrium Data and Thermodynamic Modelling of Cyclopentane and Neopentane Hydrates. *Fluid Phase Equilib.* **1997**, *138*, 241–250.

(9) Sun, Z.-G.; Fan, S.-S.; Guo, K.-H.; Shi, L.; Guo, Y.-K.; Wang, R.-Z. Gas Hydrate Phase Equilibrium Data of Cyclohexane and Cyclopentane. *J. Chem. Eng. Data* **2002**, *47*, 313–315.

(10) Jin, Y.; Kida, M.; Nagao, J. Structure H (sH) Clathrate Hydrate with New Large Molecule Guest Substances. *J. Phys. Chem. C* **2013**, *117*, 23469–23475.

(11) Takeya, S.; Ohmura, R.; Phase Equilibrium for Structure II Hydrates Formed with Krypton Co-Existing with Cyclopentane, Cyclopentene, or Tetrahydropyran. *J. Chem. Eng. Data* **2006**, *51*, 1880–1883.

(12) Imai, S.; Miyake, K.; Ohmura, R.; Mori, Y.H. Phase Equilibrium for Clathrate Hydrates Formed with Difluoromethane or Krypton, Each Coexisting with Fluorocyclopentane. *J. Chem. Eng. Data* **2006**, *51*, 2222–2224.

(13) Takeya, S.; Yasuda, K.; Ohmura, R. Phase Equilibrium for Structure II Hydrates Formed with Methylfluoride Coexisting with Cyclopentane, Fluorocyclopentane, Cyclopentene, or Tetrahydropyran. *J. Chem. Eng. Data* **2008**, *53*, 531–534.

(14) Imai, S.; Okutani, K.; Ohmura, R.; Mori, Y.H.; Phase Equilibrium for Clathrate Hydrates Formed with Difluoromethane+Either Cyclopentane or Tetra-*n*-Butylammonium Bromide. *J. Chem. Eng. Data* **2005**, *50*, 1783–1786.

Table 1. Information on the Chemicals Used in the Present Study

chemical name	source	mole fraction purity
methane	Liquid Gas Co., Ltd.	> 0.9999
fluorocyclopentane	SynQuest Laboratories, Ltd.	> 0.9869
chlorocyclopentane	Wako Pure Chemical Ind., Ltd.	> 0.98
bromocyclopentane	Merck Ltd.	> 0.99
water	Wako Pure Chemical Ind., Ltd.	> 0.9999

Table 2. Four-Phase Equilibrium Conditions (Temperature T , Pressure, p) for $\text{CH}_4+c\text{-C}_5\text{H}_9\text{X}$ (X = F, Cl, and Br)+Water Systems^a

T / K	p / MPa	T / K	p / MPa	T / K	p / MPa
CH ₄ + <i>c</i> -C ₅ H ₉ F+water system		CH ₄ + <i>c</i> -C ₅ H ₉ Cl+water system		CH ₄ + <i>c</i> -C ₅ H ₉ Br+water system	
283.17	0.03	274.24	1.11	274.17	1.82
284.17	0.08	274.37	1.13	275.15	2.03
285.12	0.14	275.24	1.28	276.19	2.32
286.12	0.21	276.11	1.46	277.13	2.61
287.21	0.29	276.98	1.65	278.12	2.93
288.18	0.38	277.48	1.77	279.15	3.30
289.17	0.49	277.89	1.93	280.05	3.65
290.16	0.60	278.74	2.11	281.12	4.15
291.14	0.74	279.73	2.42	282.10	4.68
292.14	0.90	280.59	2.71	282.61	5.00
293.12	1.07	281.20	2.98	283.18	5.45
294.14	1.28	281.91	3.29	284.12	6.03
295.13	1.52	282.68	3.68	285.11	6.87
296.10	1.79	283.47	4.09	286.14	7.92
297.09	2.10	284.55	4.72	287.15	9.08
298.19	2.51	284.15	4.54	287.74	9.93
299.16	2.92	285.14	5.17		
300.14	3.41	286.16	5.99		
301.11	3.98	287.10	6.85		
302.12	4.65	288.19	8.01		
303.11	5.44	289.19	9.33		
304.12	6.37				
305.10	7.46				
306.19	8.93				

^a Uncertainties u are $u(T) = 0.02$ K and $u(p) = 0.02$ MPa.

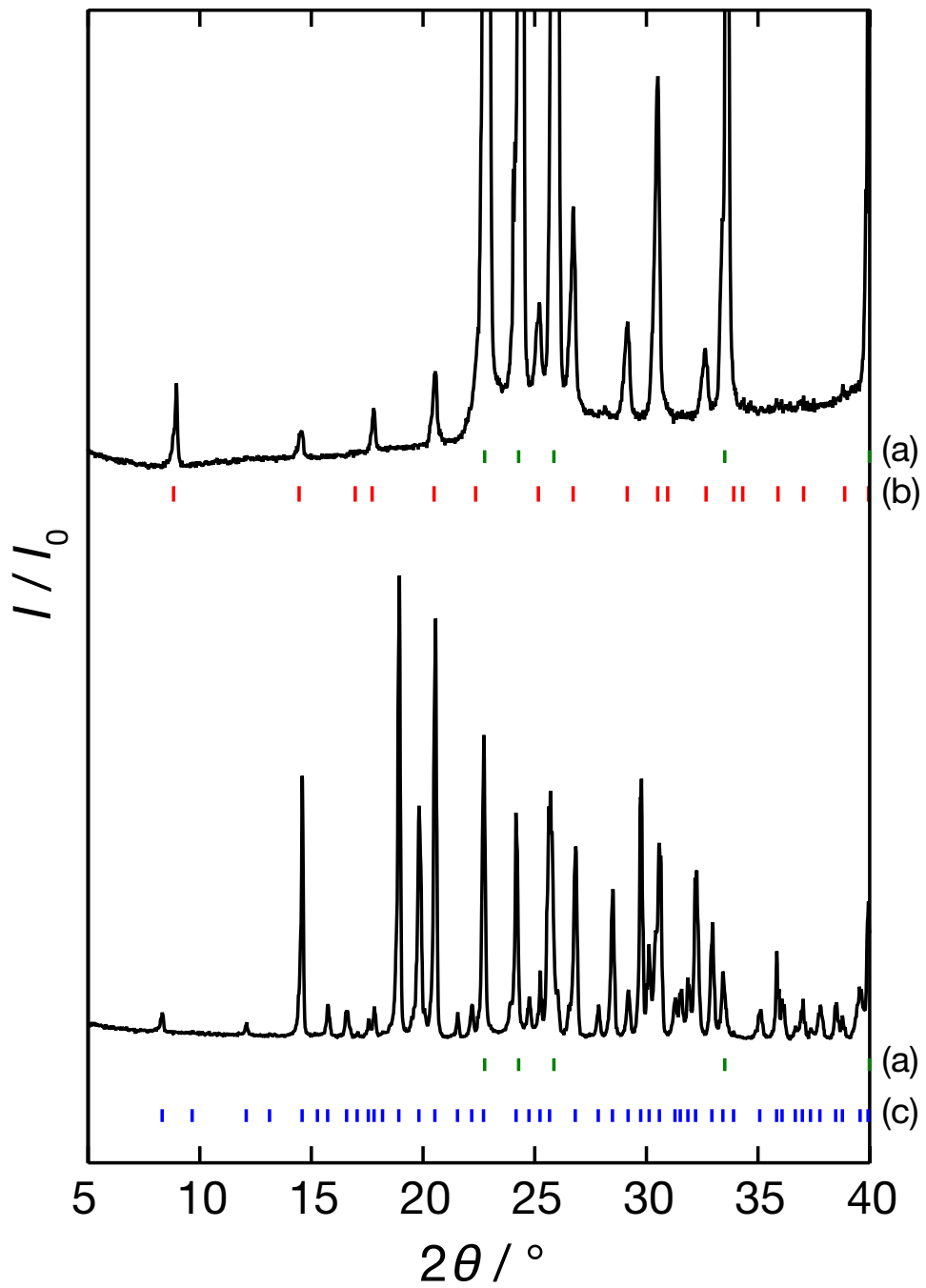


Figure 1. PXRD patterns (Intensity I , Diffraction angle θ) obtained from $\text{CH}_4 + c\text{-C}_5\text{H}_9\text{Cl}$ (upper) and $\text{CH}_4 + c\text{-C}_5\text{H}_9\text{Br}$ (bottom) mixed hydrate samples prepared in the present study (recorded at 143 K). The vertical bars represent the contributions from (a) ice Ih, (b) s-II hydrate, and (c) s-H hydrate.

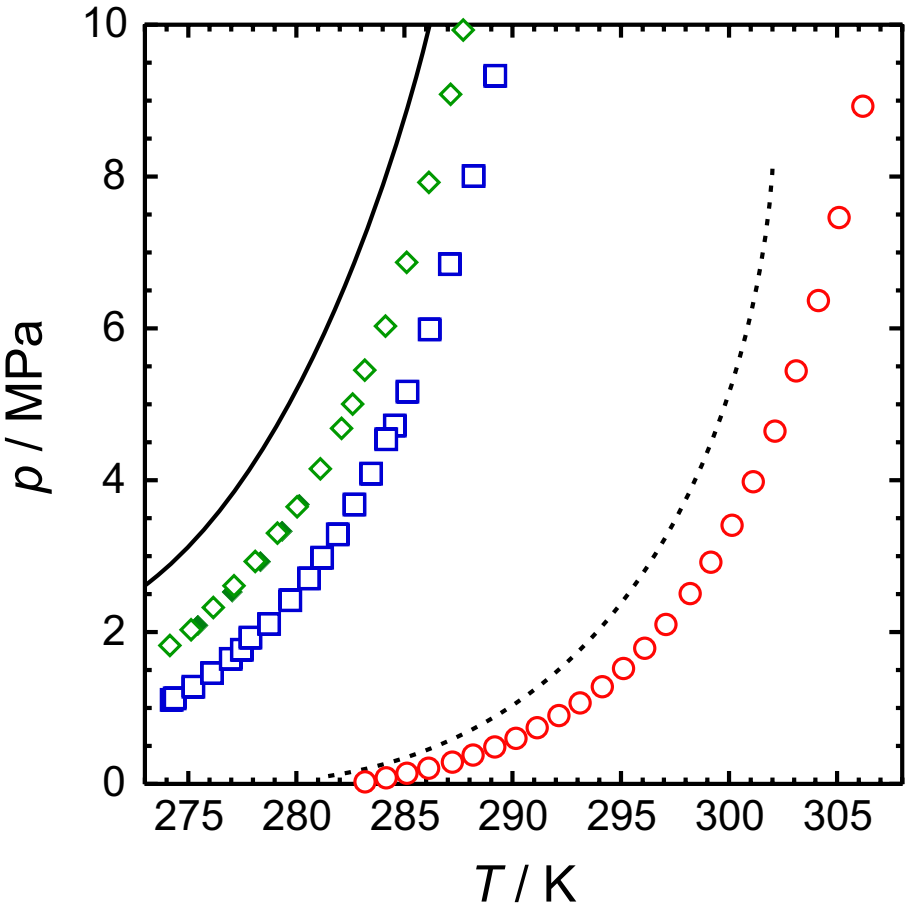


Figure 2. Four-phase (hydrate, aqueous, *c*-C₅H₉X-rich liquid, and gas phases) equilibrium relations (Temperature T , Pressure p) in the CH₄+*c*-C₅H₉X (X = F, Cl, and Br)+water ternary systems. Open circles, squares, and rhombuses stand for the four-phase (hydrate, aqueous, *c*-C₅H₉X-rich liquid, and gas phases) equilibrium relations in the CH₄+*c*-C₅H₉F+water, CH₄+*c*-C₅H₉Cl+water, and CH₄+*c*-C₅H₉Br+water systems measured in the present study, respectively. Solid curve stands for the three-phase (hydrate, aqueous, and gas phases) equilibrium curve in the simple CH₄ hydrate system.⁵ Dotted curve stands for the four-phase (hydrate, aqueous, *c*-C₅H₁₀-rich liquid, and gas phases) equilibrium curve in the CH₄+*c*-C₅H₁₀+water system.^{8,9} Solid rhombuses stand for the four-phase (hydrate, aqueous, *c*-C₅H₉Br-rich liquid, and gas phases) equilibrium relations in the CH₄+*c*-C₅H₉Br+water system.¹⁰

